Part V

Magnetic Fields, Molecular Clouds, and Interstellar Bubbles

https://doi.org/10.1017/S0252921100071037 Published online by Cambridge University Press

Carried away: The Local Bubble ...

... and some participants.

https://doi.org/10.1017/S0252921100071037 Published online by Cambridge University Press

The Magnetic Field Near the Local Bubble

Carl Heiles

University of California, Berkeley, CA 94720, USA

Abstract. There are almost no direct observational indicators of the magnetic field inside the local bubble. Just outside the bubble, the best tracers are stellar polarization and HI Zeeman splitting. These show that the local field does not follow the large-scale Galactic field. Here we discuss whether the deformation of the large-scale field by the local HI shells is consistent with the observations. We concentrate on the Loop 1 region, and find that the field lines are well-explained by this idea; in addition, the bright radio filaments of Radio Loop 1 delineate particular field lines that are "lit up" by an excess of relativistic electrons.

1 Introduction: What Deforms the Local Magnetic Field?

The magnetic field inside the local bubble is very difficult to observe. There is not a single pulsar inside the local bubble for which Faraday rotation has been measured, nor are there any neutral clouds with which to measure Zeeman splitting. Although there are some observations of the polarization of nearby stars, they are all presented in tabular form except for Tinbergen's (1982) Figure 6 (see also Frisch 1991). This figure shows that stars within about 20° of $(l, b) \sim (0°, -10°)$ have polarizations that are consistent with both the direction of the local large-scale Galactic field (i.e., with field pointing towards $l \sim 90°$) and, also, that field as it would be deformed by the North Polar Spur shell (see below). As we have heard at this meeting, there are models for the heliopause that predict a particular local field strength and orientation, but apart from the field orientation given by Tinbergen's map (which agrees with the prediction) there are no observational checks.

The magnetic field outside the local bubble is much easier to observe, most conveniently at high Galactic latitudes. Starlight polarization provides the plane-of-the-sky orientation (but not the direction) of $B_\perp$ weighted by extinction, synchrotron polarization provides the same for the radio-continuum-emitting regions, pulsar Faraday rotation and dispersion provide the mean line of sight field strength and direction $B_{||}$ for the Warm Ionized Medium (WIM), and Zeeman splitting provides $B_{||}$ in HI regions.

One of these four indicators, synchrotron polarization, is useful only if the Faraday rotation measure (RM) is known well enough, which is probably not the case in most regions. Consider the North Polar Spur as a well-studied example. Spoelstra (1971) mapped the RM's from polarization measurements of the diffuse radio continuum emission at several frequencies and found good

https://doi.org/10.1017/S0252921100071037 Published online by Cambridge University Press

agreement in the orientation of $B_\perp$ with starlight polarization for $b \gtrsim 40°$, but not at lower latitudes. However, his later map (Spoelstra 1984) of the radio polarization is based on a redetermination of the RM and doesn't allow this conclusion so clearly. In our opinion, the uncertainties in RM are too large to make a definitive statement.

We are left with starlight polarization, Zeeman splitting, and pulsar RM's. The local field, i.e. the field just outside the local bubble, differs from the large-scale Galactic field and has large-scale patterns that are correlated over fairly large angular scales, some tens of degrees.

Here we make a first attempt to quantitatively consider the following broad question: can this local magnetic field structure be explained as the large-scale Galactic field having been deformed by the local shells? This question was answered in semiquantitative terms by Weaver (1979), who eloquently described what we have in mind: "*... The numerous massive stars in the newly formed [Sco-Cen] association produced strong stellar winds. These inflated a bubble of gas and dust concentric with the Sco-Cen Association... stretched on the surface of the bubble into the filaments [and magnetic field lines] we see today...*"

This broad question, in turn, consists of four subsidiary ones. We provide the quick answers here, as we pose the questions, and elaborate in more detail below.

(1) *Question:* How do we best define the local shells? *Quick answer:* By HI maps at constant velocity, not by radio continuum loops.

(2) *Question:* What is the large-scale Galactic field? *Quick answer:* The mean magnetic field $\langle B_{||} \rangle \sim 2.2$ μG and points towards $(l, b) \sim (80°, 0°)$. The total field strength is much larger, $B_t \sim 4.2$ μG: the random field B_r dominates.

(3) *Question:* What are the observational data for the local field? *Quick answer:* Deformation of the field by shells produces easily recognizable fluctuations in the orientation of $B_\perp$ but not in the direction of $B_{||}$. This makes starlight polarization the best tracer of deformations, and they show clear disagreements with the orientation of the large-scale Galactic field $B_\perp$.

(4) *Question:* Do the local field data agree with the large-scale field as deformed by the local shells? *Quick answer:* Here we concentrate on the North Polar Spur: the agreement is very good in some regions, and the strongly emitting ridges in Radio Loop I follow the distorted field lines very well.

2 How Should We Define the Local Shells?

2.1 With Radio Continuum—No!

The four classical radio continuum loops are usually interpreted as the major tracers of large, local supernova shells (Berkhuijsen, Haslam, and Salter 1971). However, I want to emphasize that *with the exception of Radio Loop 1, none*

https://doi.org/10.1017/S0252921100071037 Published online by Cambridge University Press

of these radio loops looks like a limb-brightened shell. The arcs of Radio Loops 2, 3, and 4 are fat, with radial extents that are $\sim 1/3$ the loop radius. If they were limb-brightened shells, then the intensities inside the peripheries would be almost as large as those in the limb-brightened parts—but this is not the case. As we discuss below, Radio Loop 1 does have a brighter interior and is to some extent a limb-brightened shell, but it also exhibits a number of roughly concentric filaments at various radial distances inside its periphery, something that is difficult to achieve with nothing but limb brightening, even with a wrinkled boundary.

Furthermore, the radio loops are not reliable indicators of supernova shells. Radio Loop 1 is the most famous loop and it is certainly tracing a supernova shell which also exhibits a very well-defined expanding HI shell, soft X-ray emission from the interior, and an obvious structure in the famous map of starlight polarization by Mathewson and Ford (1970). However, the Eridanus loop also has the HI shell and X-ray emission and therefore deserves equal billing as a supernova shell—but it does *not* exhibit a well-defined radio loop structure. Finally radio loops 2, 3, and 4 have no reason, other than their radio continuum emission, to be billed as supernova shells. Moreover, these three loops are not very distinct, and there are a few other radio features that are just as clear but not classified as loops, one of the clearest having diameter $\sim 50°$ and centered near $(l, b) = (280°, -30°)$ (close to the Large Magellanic Cloud—almost certainly a pure accident!).

We conclude that the radio continuum loops are not very good tracers of interstellar shell structures, nor are they limb-brightened shells.

2.2 With HI—Yes!

Defining shells with the HI makes physical sense. The HI gas is affected strongly by stellar winds and supernova explosions. It expands, sweeping up the magnetic field with it into a shell; it slows down and stalls, with the HI remaining as a tracer until other shocks come along and jostle it again. HI shells become very clear and distinct in maps at different velocities. The grey-scale HI maps of Colomb, Pöppel, and Heiles (1980), as crude and poorly reproduced as they are, reveal a plethora of well-defined shells. The field strength $B_{||}$ in this neutral gas is derivable from HI Zeeman splitting and the orientation of $B_{\perp}$ from starlight polarization.

3 The Large-Scale Galactic Field

The recent least square fits to pulsar data by Rand and Lyne (1994) find $\langle B \rangle \equiv B_u \sim 1.4\ \mu$G, pointed towards $l \sim 88°$. However, while these results are most popular, they differ from those obtained from two indicators that sample larger volume fractions of space, synchrotron polarization and

https://doi.org/10.1017/S0252921100071037 Published online by Cambridge University Press

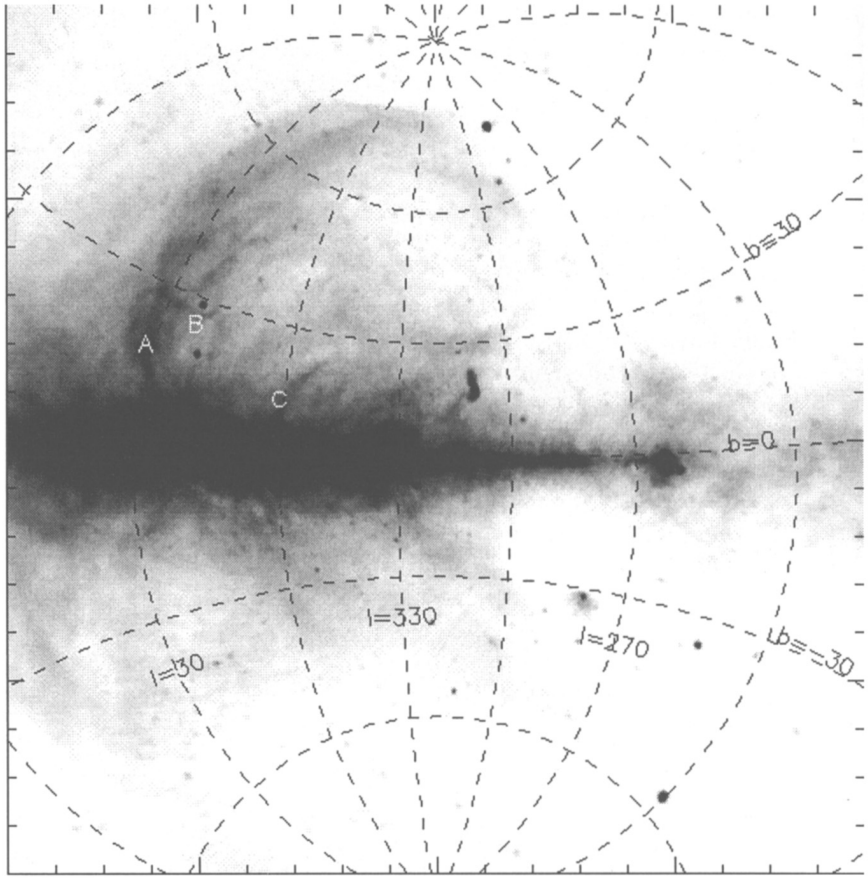

Fig. 1. The 408 MHz radio continuum from Haslam *et al.* (1983) (grey scale) and Galactic coordinate grid, in stereographic projection centered on $(l, b) = (320°, 5°)$. The dashed lines are lines of constant Galactic longitude and latitude in intervals of 30°. The letters A, B, and C label particular bright filaments discussed in the text.

starlight polarization. These more representative indicators provide $B_u \sim 2.2$ μG, pointed towards $l \sim 80°$ (Heiles 1995, 1996).

The random field strength B_r much exceeds the uniform component B_u, but by a factor that depends on whether the data are RM's (from the WIM) or other non-WIM indicators. Ohno and Shibata (1993) analyzed pulsar RM's and found $\frac{B_u}{B_r} \sim 0.28$. In contrast, the non-WIM $\frac{B_u}{B_r}$ as derived from starlight polarization (Jones, Klebe, and Dickey 1992) and synchrotron emissivity is at least twice as large. Moreover, the scale lengths for the random field variations differ, being much smaller in the WIM. Heiles (1995) considers all these data

https://doi.org/10.1017/S0252921100071037 Published online by Cambridge University Press

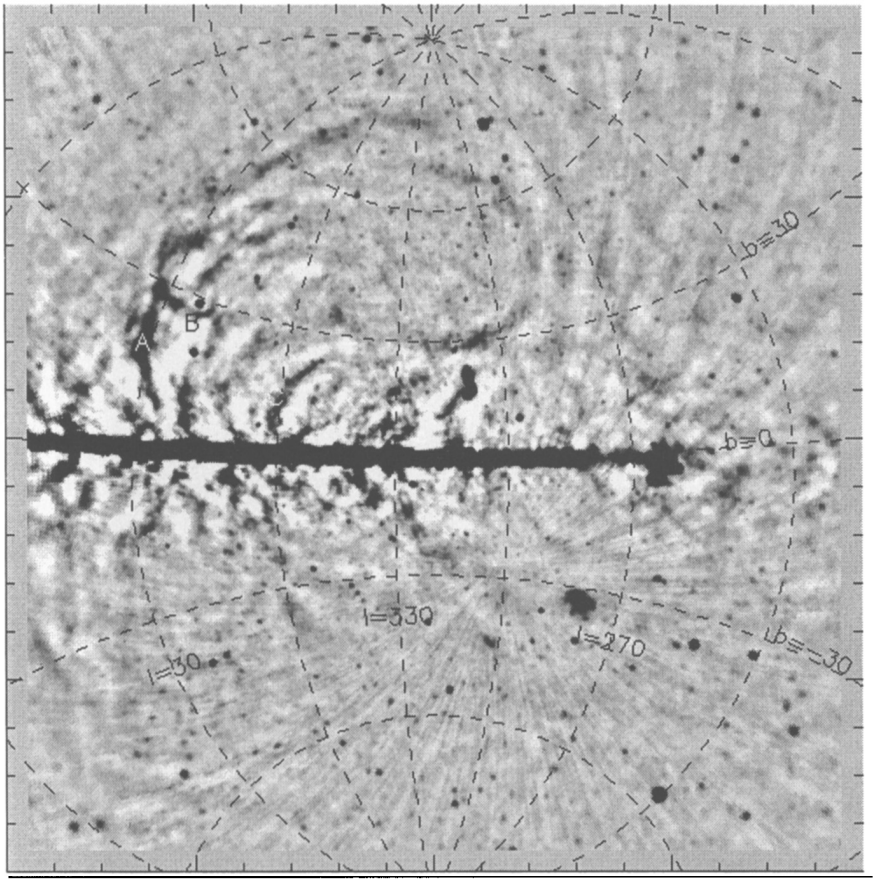

Fig. 2. High-pass filtered 408 MHz radio continuum; blacker is brighter. The stereographic projection and letters A, B, and C are identical to Figure 1.

together and believes that the pulsar data should receive less weight than they are usually given.

The RM data show disturbing large-scale residuals from the least square fit to the large-scale Galactic field. In Galactic quadrant 1 at $b > 0°$, the RM's are almost uniformly positive; in contrast, from the least square fit they should be negative. A similar situation holds for quadrant 3 at $b < 0°$. This disturbing discrepancy is the subject of a paper by Han et al (1997), who ascribe it to a large-scale Galactic dipole field caused by a dynamo of odd symmetry. However, the HI Zeeman splitting data—although they are too sparse to say definitively—do not seem to exhibit this discrepancy: the signs of the Zeeman-derived $B_{||}$ agree better with those of the large-scale

https://doi.org/10.1017/S0252921100071037 Published online by Cambridge University Press

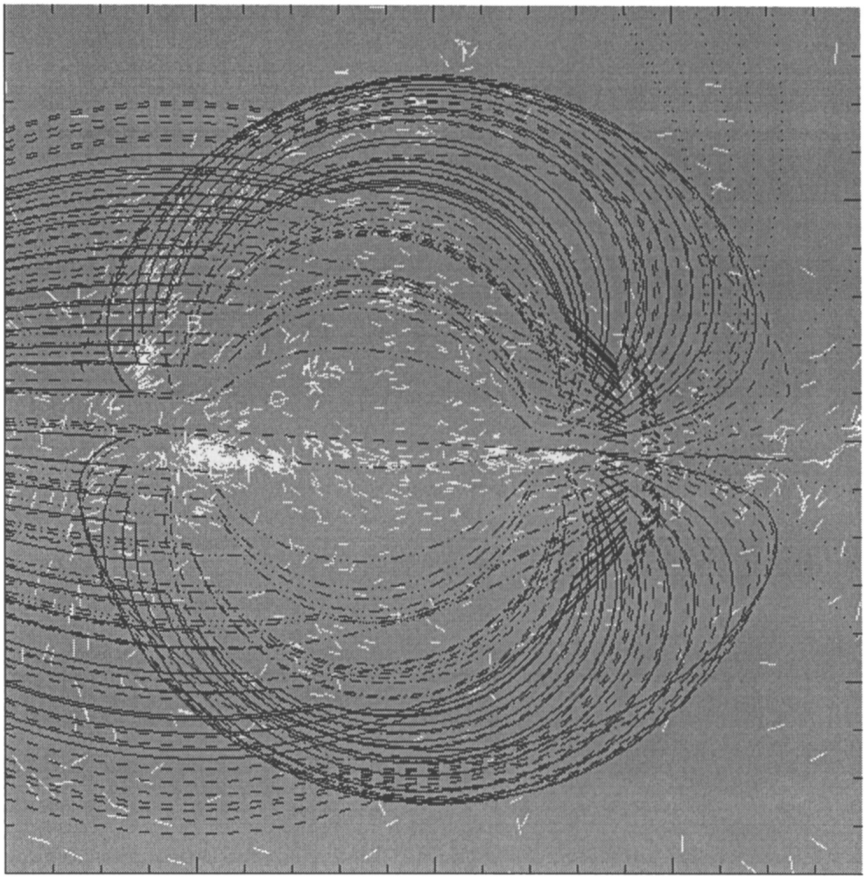

Fig. 3. The white "vectors" are starlight polarizations. The black lines represent our model of magnetic field lines deformed by the expanding HI shell, with the line type indicating the distance: the nearest field lines are dotted, then dashed, then solid, then dash-dot-dot, and the furthest dash-dot-dot-dot. The stereographic projection and letters A, B, and C are identical to Figure 1.

fit. Similarly, for the NPS deformed field model discussed below, the Zeeman splitting data agree well and the RM data do not.

Again, we believe that the WIM is not the best magnetic field tracer in most regions. In any case, for our problem of the deformed field in shells the starlight polarization results must be more relevant because they refer mainly to the HI shells, while the RM data refer to the WIM—which is not very well-correlated with the HI (Reynolds et al 1995). Thus we will ignore the RM data in the present discussion.

https://doi.org/10.1017/S0252921100071037 Published online by Cambridge University Press

4 The Local Field as Distorted by the North Polar Spur

When an expanding spherical shell deforms field lines, the deflected lines follow lines of constant "longitude" on the sphere. Their appearance on the sky depends on the vantage point, like viewing the constant-longitude lines on a terrestrial globe from different vantage points.

When observed from the "magnetic pole" the spherically-deflected lines project radially onto the sky, and the deflections change neither the orientation of $B_\perp$ nor the sign of $B_{||}$. When observed from the "magnetic equator" the deformed lines look straight near the center and change gradually to being circumferential near the limbs; the undeformed $B_{||}$ is small, but the deformed $B_{||}$ is positive or negative depending on whether one observes the front, rear, left, or right hemispheres. From other vantage points the geometry becomes complicated, with surprising consequences. For example, field lines on the rear hemisphere can be almost perpendicular to those on the front. If the sphere subtends a large angle then the geometrical projections make things even more complicated. Some of these effects are visible in Heiles' (1997) study of the field structure in the Orion/Eridanus region and below in Figure 3.

Here we do not have enough space to discuss all the radio loops, so we concentrate on the physical structure associated with Radio Loop 1. Because this structure encompasses more than just the radio emission, we call the whole structure, including the radio loop, the "North Polar Spur" or NPS. Just outside of the radio loop lies the periphery of an expanding HI shell; in contrast to the radio loop, the HI shell extends below the Galactic plane to $b \sim -30°$. From an eyeball fit, the HI shell is centered near $(l, b) = (320°, 5°)$, significantly different from the radio loop center $(l, b) = (329° \pm 1.5°, 17.5° \pm 3°)$ (Berkhuijsen, Haslam, and Salter 1971). The fact that the HI center is lower than the radio center, and in particular as low as $b \sim 5°$, is important in our following discussion, where we match the pattern of deformed field lines to the bright filaments in Radio Loop 1.

Figure 1 shows a stereographic map of the 408 MHz radio continuum from the survey of Haslam *et al.* (1983), with a Galactic coordinate grid superposed. The stereographic projection is ideal for examining shells because it always maps circles into circles (but usually with displaced centers). The most intense radio emission arches up towards positive latitudes near $l \sim 30°$ and there are several roughly concentric filaments of different radius. The filaments lie roughly parallel to the stellar polarization (see Figure 3), suggesting that the filaments trace magnetic field lines. The letters A, B, and C trace particular bright radio filaments that we will discuss below.

We can highlight the radio filaments by using a high-pass filter ("unsharp masking") on the image, which rejects the broad background; this is shown in Figure 2, where blacker means more intense.

https://doi.org/10.1017/S0252921100071037 Published online by Cambridge University Press

Figure 3 exhibits the large-scale Galactic field lines as they would be deformed by the expanding HI NPS shell. In this model, we assume that each unperturbed field line, with the gas, is swept up by the shock into the shell along a radial line emanating from the shell center at $(\ell, b) = (320°, 5°)$. The distances of the field lines from the Sun are indicated by their type, as explained in the figure caption.

We see that the pattern of radio filaments looks very similar to the pattern of the deformed lines, particularly near the upper left periphery of the shell. In particular, the sharp bend in the radio filament just above the letter B, where the deformed lines bend sharply from being nearly vertical to being horizontal as they approach the Galactic plane from above, is reproduced well.

This pattern matching, plus the many bright filaments that exist not only near the periphery, suggests that the bright radio filaments trace particular distorted magnetic field lines. This is a very strong indication that the brighter portions of Radio Loop 1 are not bright because of limb brightening. Rather, they are defined by distorted field lines that happen to be "lit up" by relativistic electrons. Whatever the physical cause, the effect is huge: the mean Galactic synchrotron emissivity near the Sun is ~ 7 K kpc^{-1} (Beuermann, Kanbach, and Berkhuijsen 1985) and the the bright filaments have at least several Kelvins pc^{-1}, $\gtrsim 500$ times higher!

It would be nice to find some reason why particular field lines are lit up by relativistic electrons. It may be that the bright lines are those that happen to run near dense regions, perhaps where the shock associated with the expanding HI shell traps and accelerates relativistic electrons more effectively. Dense gas clouds are highlighted by diffuse 100 μm IRAS emission, which is shown in Figure 4.

In Figure 1 we marked two of the brightest field lines with the letters A and C. Field line A is the brightest. It is morphologically similar to a fairly weak, but nevertheless distinct, feature on the 100 μm IRAS map. This IRAS feature lies outside the corresponding radio continuum feature, so we regard the association as "probable" but not definite. Comparison of the IRAS map with HI data shows that this feature has a velocity in the range $12 \rightarrow 22$ km s^{-1}, which places it somewhat beyond the tangent point of the HI shell; field lines at this distance (and also other distances) also have this bend. Similarly, field line C runs over a very bright feature on the IRAS map; this feature is the Ophiuchus molecular cloud region. This association of IRAS and radio is much clearer and we can regard it as "definite", although the pattern of distorted field lines in Figure 3 does not match very well. Ophiuchus has a velocity $\sim +8$ km s^{-1} and therefore lies on the far side of the HI shell.

The associations (one "probable", one "definite") of the bright radio filaments with these dense gas features suggests that the particular field lines that lie near the interaction region that exists between particular dense pock-

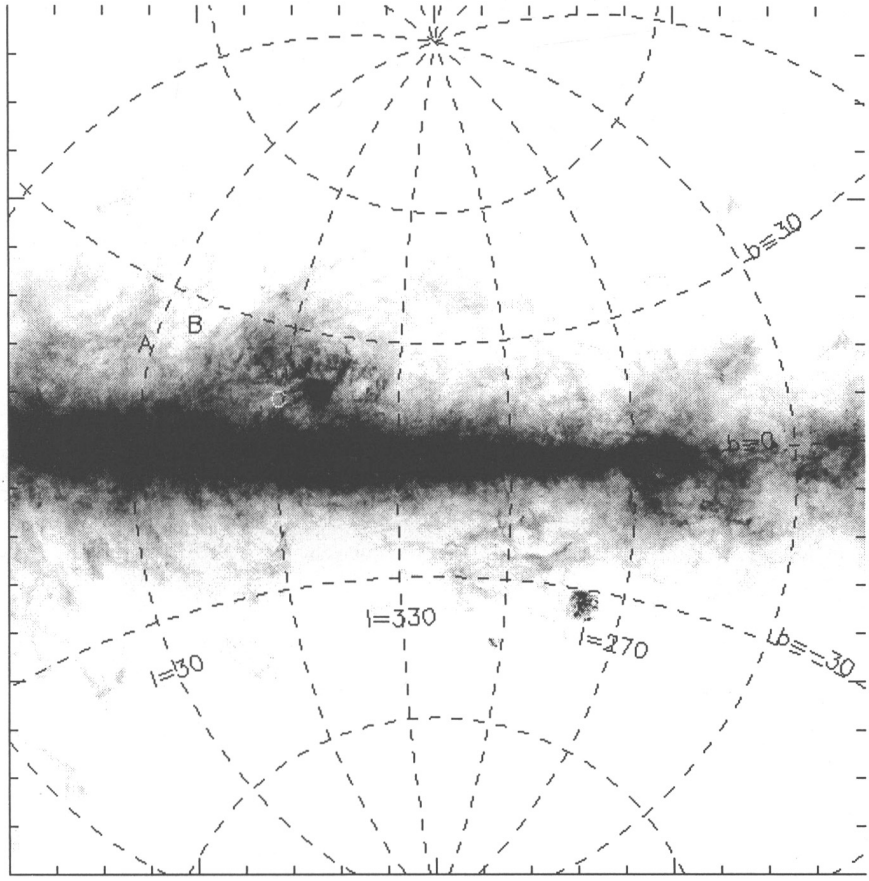

Fig. 4. Diffuse 100 μm IRAS emission. The stereographic projection and letters A, B, and C are identical to Figure 1.

ets of gas and the expanding shock are the ones where relativistic electron generation occurs particularly efficiently.

Finally, Figure 3 shows that the starlight polarization is well represented by the distorted field lines for $b \gtrsim 0°$ in the left-hand half of the NPS. This is encouraging as a positive answer to our fundamental question.

Acknowledgements. It is a pleasure to thank Doug Finkbeiner for his diffuse 100 μm IRAS map and his assistance in using it, and Dap Hartmann for assistance in using his Dwingeloo HI survey. This work was supported by a grant to the author from the National Science Foundation.

References

Berkhuijsen, E.M., Haslam, C.G.T., Salter, C.J. (1971): A&A, 14, 252
Beuermann, K., Kanbach, B., and Berkhuijsen, E.M. 1985, A&A, 153, 17
Colomb, F.R., Pöppel, W.G.L., and Heiles, C. (1980): A&AS 40, 47
Frisch, P.C. (1991): in *COSPAR Colloquia Series No. 1, Physics of the Outer Heliosphere*, S. Grzedzielski and E. Page (eds.), (London: Pergamon), p. 19
Han, J.L., Manchester, R.N., Berkhuijsen, E.M., and Beck, R. (1997): A&A, in press
Haslam, C.G.T., Salter, C.J., Stoffel, H., & Wilson, W.E. 1983, A&AS, 47, 1
Heiles, C. (1995): in *Polarimetry of the Interstellar Medium*, ASP Conference Series Volume 97, ed. W.G. Roberge and D.C.B. Whittet, p. 457
Heiles, C. (1996): ApJ, **462**, 316
Heiles, C. (1997): ApJS, in press
Jones, T.J., Klebe, D., and Dickey, J.M. (1992): ApJ, **389**, 602
Mathewson, D.S. and Ford. V.L. (1970): Mem. R. Astron. Soc., **74**, 139
Ohno, H. and Shibata, S. (1993): MNRAS, **262**, 953
Rand, R.J. and Lyne, A.G. (1994): MNRAS, **268**, 497
Reynolds, R.M., Tufte, S.L., Kung, D.T., McCullough, P.R., and Heiles, C. (1995): ApJ, **448**, 715
Spoelstra, T.A.Th. (1971): A&A, **21**, 85
Spoelstra, T.A.Th. (1984): A&A, **135**, 238
Tinbergen, J. (1982): A&A, **105**, 53
Weaver, H.F. (1979): in *The Large-Scale Characteristics of the Galaxy*, ed. W.B. Burton, p. 295